Motor Control After Human SCI Through Activation of Muscle Synergies Under Spinal Cord Stimulation

Richard Cheng, Yanan Sui, Dimitry Sayenko, and Joel W. Burdick

***Abstract*— Spinal cord stimulation (SCS) has enabled motor recovery in paraplegics with motor complete spinal cord injury (SCI). However, the physiological mechanisms underlying this recovery are unknown. This paper analyzes muscle synergies in two motor complete SCI patients under SCS during standing and compares them with muscle synergies in healthy subjects, in order to help elucidate the mechanisms that enable motor control through SCS. One challenge is that standard muscle synergy extraction algorithms, such as non-negative matrix factorization (NMF), fail when applied to SCI patients under SCS. We develop a new algorithm–rShiftNMF–to extract muscle synergies in these cases. We find muscle synergies extracted by rShiftNMF are significantly better at interpreting electromyography (EMG) activity, and resulting synergy features are more physiologically meaningful. By analyzing muscle synergies from SCI patients and healthy subjects, we find that: 1) SCI patients rely significantly on muscle synergy activation to generate motor activity; 2) interleaving SCS can selectively activate an additional muscle synergy that is critical to SCI standing; and 3) muscle synergies extracted from SCI patients under SCS differ substantially from those extracted from healthy subjects. We provide evidence that after spinal cord injury, SCS influences motor function through muscle synergy activation.**

***Index Terms*— Muscle synergy, spinal cord stimulation (SCI), spinal cord injury (SCI), matrix factorization, electromyography (EMG).**

I. Introduction

MOTOR activity requires a complex mapping from the brain to the spinal cord and then to individual muscles. In 1994, Mussa-Ivaldi et al. observed that in frogs, total muscle activity was encoded as a linear superposition of a few motor primitives, suggesting a low-dimensional, linear representation of motor output [1]. *Muscle synergies* capture these motor primitives and represent the low-dimensional, linear motor behavior [2]–[4]; they are defined as the coordinated recruitment of a group of muscles with a specific activation signal. The idea is that each muscle synergy represents a network of neurons activated by a single neural command. Each neuronal network excites a specific pattern of motoneurons, resulting in fixed patterns of muscle activity following a similar activation signal. A current theory is that the spinal cord controls functional motor activity, in large part, by modulating activity of muscle synergies – rather than controlling individual muscles [5]. These muscle synergies constitute a feedforward drive, but may incorporate closed-loop control mechanisms dependent on peripheral sensory input [4], [6]. Fig. 1 illustrates two muscle synergies contributing to electromyography (EMG) activity.

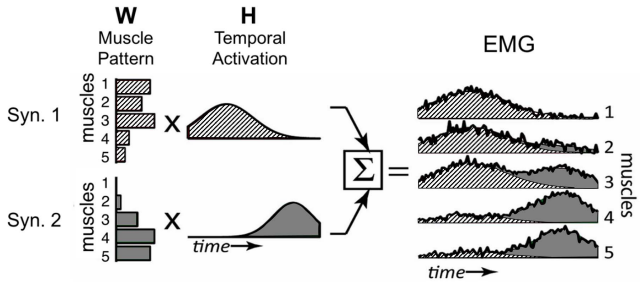

Fig. 1. Illustration of two muscle synergies composed to reconstruct EMG activity. W represents the muscle activation pattern, and H represents the activating neural signal for two different muscle synergies. This figure was adapted from [7].

Animal studies provide substantial evidence for muscle synergies encoded in the spinal cord. When stimulating different parts of the spinal cord together or separately (electrically or chemically), researchers have observed that resulting motor activity from joint stimulation is approximately a linear combination of the motor activity induced by separate stimulation [8]–[12]. By measuring neuron activity in the spinal cord concurrently with muscle activity in different animals, studies suggest that muscle synergies are encoded in the spinal cord through sets of dedicated interneurons [13], [14].

Although such experiments have not been done in humans, it has been shown that human muscle activity can be accurately described by the linear superposition of a few muscle synergies [7], [11], [15]–[20]. Synergies are extracted from human EMG measurements during specific tasks (e.g. reaching, stepping, etc.), and represent low-rank approximations of the muscle activity – i.e. a small number of muscle synergies linearly combine to compose overall muscle activity.

Non-negative matrix factorization (NMF) is a widely used method for searching for this low rank approximation of muscle activity [21]. This method extracts muscle *activation*

Manuscript received November 20, 2018; revised March 20, 2019; accepted April 17, 2019. Date of publication May 2, 2019; date of current version June 6, 2019. This work was supported by the National Institute of Health (NIH) under Grant EB007615. *(Corresponding author: Richard Cheng.)*

R. Cheng and J. W. Burdick are with the Mechanical Engineering Department, California Institute of Technology, Pasadena, CA 91125 USA (e-mail: rcheng@caltech.edu).

Y. Sui is with the Computer Science Department, Stanford University, Stanford, CA 94305 USA.

D. Sayenko is with the Center for Neuroregeneration, Houston Methodist Research Institute, Houston, TX 77030 USA.

Digital Object Identifier 10.1109/TNSRE.2019.2914433

patterns W (representing the coordinated recruitment of a group of muscles) and *neural activation signals* H (representing the activation waveform that excites the specific group of muscles), which best fit the EMG data. The result is a set of muscle synergies that represent the EMG activity, and the quality of this representation can be measured by the residual error between the reconstructed EMG and measured EMG.

Tresch et al. showed that the set of muscle synergies extracted is robust to the choice of matrix factorization algorithm [22]. We focus on NMF because, in addition to good performance and robustness to noise, it ensures positive activation (a physiological assumption on muscle synergies) and does not assume orthogonality of the different synergies.

However, such algorithms have not yet been used to extract muscle synergies from patients with spinal cord injury (SCI) under spinal cord stimulation (SCS), as these cases pose additional challenges that cause the standard algorithms [22] to fail. This paper explores the existence, extraction, and control of muscle synergies in paraplegics with motor complete SCI under SCS. Recent studies have shown that motor complete SCI patients can recover significant motor function under SCS, even demonstrating overground stepping after intensive therapy [23]–[27]. However, the neural mechanisms by which this recovery is achieved are not well understood. This study aims to elucidate some of these mechanisms through analysis of muscle synergies. A recent animal study showed that targeted neuromodulation of muscle synergies in SCI rats could provide significant improvements in motor control [28]. Thus, a better understanding of muscle synergies in human SCI may lead to improved therapies.

The first section of this paper introduces a novel algorithm to extract muscle synergies from SCI patients under SCS, as standard algorithms fail due to the presence of consistent time delays between the activation of different muscle groups. The second part of this study analyzes the muscle synergy activation patterns and the number of muscle synergies induced by SCS during standing, and finds that proper stimulation can selectively activate an additional muscle synergy that produces markedly improved functional behavior. The last part of this study briefly compares muscle synergies extracted from SCI patients attempting to stand under SCS, with those extracted from healthy human subjects during quiet standing. We find that the muscle synergies resulting from SCS are significantly different from healthy muscle synergies.

The contributions of this paper are:

- Introduction and application of the rShiftNMF algorithm to enable extraction of muscle synergies in SCI patients under SCS,
- Computational evidence of intact muscle synergies in the spinal cord after SCI that are activated through SCS,
- Comparison of SCI patient muscle synergies with healthy subject muscle synergies,
- Identification of a spinal stimulation strategy that improves SCI patient standing performance via selective activation of an additional muscle synergy.

A preliminary version of this work appeared in [29], but focused on the rShiftNMF algorithm for synergy extraction.

II. Methods

A. Experiments

1) SCI Patient Trials: Data was collected from two complete (ASIA A), paraplegic SCI patients implanted with a Medtronic 5-6-5 epidural electrode array for SCS with a Medtronic RestoreAdvanced Neurostimulator. The 16-electrode array was implanted over the spinal cord segments L1-S1. The patients (referred to as patients A and B) gave their written informed consent to participate in the study, whose experimental procedures were approved by the local ethics committee. For patient A, experiments were performed over two non-consecutive weeks, six months apart, and a total of 109 trials of stimulation/EMG data were gathered (we'll refer to the earlier week as session 1 and the later week as session 2). For patient B, experiments were performed over one week, and a total of 15 trials of stimulation/EMG data were gathered. Before the first experiments were done, the patients underwent 80 sessions of intensive stand training (1 hour, 5 sessions per week) under SCS, in which they were encouraged to stand for as long as possible with the least amount of assistance.

The choice of stimulating electrodes recruited on the array and their polarities (i.e. the stimulation patterns) were modified between trials. This choice was determined by a machine learning algorithm, which continually proposed different "safe" stimuli (high probability of eliciting non-painful response), and continually tested good ones against each other to search for the optimal stimulation patterns (resulting in independent standing) [30], [31]. Stimulation frequency and pulse width were kept constant between trials at 25 Hz and 200 μs, respectively. For a fixed stimulation pattern, frequency, and pulse width, SCS amplitude was ramped upward until reaching a well-performing value.

For four of the experimental trials with patient A and one of the trials with patient B, rather than using a single fixed stimulation pattern, 4 different stimulating patterns were interleaved together in a sequence with a frequency of 10 Hz. Therefore, the stimulation pattern was time-varying (changing every $\approx 25ms$), and the 4 chosen stimulation patterns would repeat every 100 ms. We will refer to these time-varying stimuli as *interleaving stimulation*. Empirically well-performing stimulation was used for each of the 4 patterns.

During each trial, the patient attempted to stand with minimal support for 1 to 5 minutes under spinal stimulation. The patient achieved full weight-bearing standing with no assistance when empirically-optimal stimulating configurations were used. *Neither patient could achieve leg muscle control or report any sensory function without stimulation.*

We utilized measurements from 10 muscles (5 muscle groups) taken using sEMG (surface electromyography) at a sampling frequency of 2000 Hz. The 5 muscle groups were: VL (vastus lateralis), MH (medial hamstring), MG (medial gastrocnemius), TA (tibialis anterior), and SOL (soleus). The EMG was high-pass filtered at 3 Hz, rectified, and low-pass filtered at 30 Hz using a 5th order butterworth filter.

Note that the filtering applied here is significantly less aggressive (retains a much larger signal bandwidth) than the pre-process filtering typically applied to EMG in other

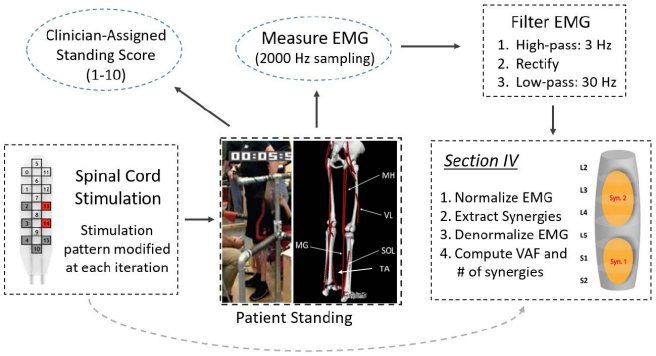

(a)

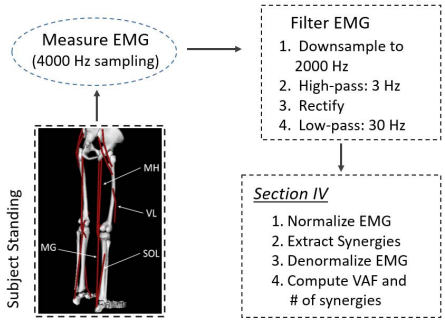

(b)

Fig. 2. Experimental procedure for stimulation, data collection, and analysis for (a) SCI patients and (b) healthy subjects.

muscle synergy studies. For example, the high-pass and low-pass filter cutoff frequencies are set at 35/40 respectively in [15], or 35/35 in [16], whereas our high pass and low-pass filter cutoff frequencies are set at 3/30, respectively. Our larger-bandwidth filter is necessary to retain important structure in the EMG spectrum induced by spinal stimulation, which is highly structured in SCI patients under SCS. This allows us to analyze detailed phenomenon at the muscle activation level that would otherwise be smoothed out. Figure 2a illustrates the experimental procedure for each trial.

After every trial, clinicians quantified standing quality utilizing a discrete scoring system that ranges from 1 to 10, with 1 being the worst and 10 being the best. From scores 1 to 5, the standing is not independent but requires less external assistance as the score increases. From scores 6 to 10, standing is overall independent and full-weight bearing. As the score increases, standing is more stable and durable.

2) Healthy Subject Trials: Data was collected from five healthy participants (age: 27.2 ± 4.5 years; height: 168 ± 9 cm; weight: 62.3 ± 10.9 kg). They had no medical history of neurological disorders. All subjects gave their written informed consent to participate in the study, whose experimental procedures were approved by the local ethics committee.

Each participant stood quietly with bare feet, eyes open, and arms hanging along the sides of the body for the duration of 60 s. The participant was instructed to stand quietly and to refrain from any voluntary movements.

We utilized measurements from 4 muscle groups (VL, MH, MG, SOL) taken using sEMG at a sampling frequency of 4000 Hz, using a PowerLab 16/35 series DAQ system. To compare results with the SCI patients, we downsampled the signal to emulate a sampling frequency of 2000 Hz, and then the EMG was high-pass filtered at 3 Hz, rectified, and then low-pass filtered at 30 Hz using a 5th order butterworth filter. Fig. 2b illustrates the experimental procedure for each subject.

B. Extraction of Muscle Synergies

The NMF algorithm developed in [21] has been used extensively to extract muscle synergies in humans and animals [5], [32]. The algorithm efficiently solves the optimization problem in Equation 1 using alternating least squares with multiplicative updates to find a local optimum.

$$\underset{W,H}{\operatorname{argmin}} \; \|EMG - \sum_{d} W_{n,d} H_{d,t}\|^2 \tag{1}$$

In Equation 1, EMG refers to the rectified and filtered EMG signal – an N-by-T matrix composed of N signals (1 for each muscle) of length T. $W_{n,d}$ represents the activation pattern of each muscle synergy where n indexes each of the N muscles, and d indexes each of the D muscle synergies (i.e. each column represents the muscle activation pattern for synergy d). $H_{d,t}$ represents the activating signal for each muscle synergy where t indexes each time step of the activating signal, and d indexes each of the D muscle synergies (i.e. each row represents the activating signal for synergy d). This is illustrated in Fig. 1.

However, analyzing muscle synergies in SCI patients under SCS introduces a unique challenge, which causes NMF to perform poorly in these cases. It is known that neural activation signals take differing times to reach different muscles, based on conduction delays along axons. In patients with SCI under spinal stimulation, these delays are well-defined and very prominent, since an activating signal is externally induced at a specific area of the spinal cord at a fixed frequency. This activating signal must propagate through the interneuronal and motorneuron pathways down the lower limbs, resulting in measurable and diverse delays in the EMG response at distal muscles (see Fig. 3a). Therefore, extracted muscle synergies must account for these delays, which NMF cannot do. The implicit requirement imposed by the NMF algorithm for synergy extraction is that each neural signal generated by the spinal cord must reach every muscle simultaneously.

In order to account for conduction delays when extracting muscle synergies, we develop a variant of NMF that can account for continuous delays (and incorporate delay priors), referred to as rShiftNMF. The mathematical framework has parallels to time-varying synergies (TVS) [33], [34], although our experiments deal with delays on a much shorter time-scale and within the same synergy profile. To avoid confusion, we will refer to the muscle synergies extracted by rShiftNMF as Conduction-Delayed Synchronous Synergies (CDSS).

First, the NMF optimization problem is reformulated to include delays, τ, as follows in Equation 2. An algorithm for efficiently solving this problem is derived in [35].

$$\underset{W,H,\tau}{\operatorname{argmin}} \; \|EMG - \sum_{d} W_{n,d} H_{d,t-\tau_{n,d}}\|^2 \tag{2}$$

By adding a delay parameter, τ, to the original optimization problem, we allow for delays, $\tau_{n,d}$, in arrival time (of neural signal, d) at each individual muscle, n. The index (n, d) refers to the delay for muscle n in the d^{th} muscle synergy. These delays allow us to eliminate the assumption that all muscles are activated simultaneously by a given muscle synergy. The optimization problem in Equation 2 is solved by first doing a Fourier transform on the parameters W, H, τ to conveniently express the delay as multiplication by a complex exponential. Then we use alternating least squares with multiplicative updates to iteratively converge on parameter estimates [35].

However, we also must ensure that the calculated delays are consistent with neurophysiology. Since Equation 2 defines a non-convex problem, convergence to a local optima may result in non-physiological delays. Consider that a generic 10Hz periodic signal would be equally likely to have a 10ms delay and a 110ms delay. Hence, the optimization problem above may lead to non-physiological estimates of the delay τ, given that (1) many local optima exist and (2) many delays τ can lead to similarly good factorizations. However, based on the physiology of the CNS, we can estimate the order of magnitude of expected conduction delays. For example, neural signals travel down motor neurons at speeds on the order of $100\frac{meter}{sec}$, and the length of a lower limb is between 0.5 to 1 meters, so a signal sent from the spinal cord should take order of magnitude 10 milliseconds longer to reach a thigh muscle than shank muscle with patient-specific variations.

Given order of magnitude estimates of expected delays, we can modify the algorithm to incorporate a prior, $T^{prior}_{n,d}$, on the delays to ensure that the delays remain consistent with physiology. Assuming the synergy reconstruction error is Gaussian (i.e. $\mathbb{P}(EMG|W, H, \tau) = \mathcal{N}(\sum_d W_{n,d} H_{d,t-\tau_{n,d}}, \Gamma)$), then adding a Gaussian prior with mean T^{prior} on the delay, τ, in a Bayesian formulation of the problem is equivalent to adding L_2 regularization to the underlying optimization problem, as shown in Equation 3 below:

$$\underset{W,H,\tau}{\operatorname{argmin}} \|EMG - \sum_d W_{n,d} H_{d,t-\tau_{n,d}}\|^2 + \lambda \|\tau - T^{prior}\|^2. \quad (3)$$

The new optimization problem can be solved by alternating least squares as in [35], and only the update law for the delays $\tau_{n,d}$ must be modified by linearly adding in the gradient/Hessian corresponding to the regularization term. This defines the rShiftNMF algorithm (code available at https://github.com/rcheng805/rShiftNMF). We refer to synergies extracted by rShiftNMF as conduction-delayed synchronous synergies (CDSS), and those extracted by NMF as synchronous synergies (SS) [11].

In order to ensure that the effect of each muscle is balanced when dealing with the optimization, we normalize the EMG activity for each channel before running the rShiftNMF and NMF algorithms. We then de-normalize the data (i.e. re-multiply the normalization factors into W) after the synergies have been extracted, so that it accurately reflects the muscle activation pattern of the different muscles.

Note that since the rShiftNMF algorithm uses 10 more free parameters per synergy (for 10 muscles) compared with NMF, it is expected to better fit to the data. To address this, we run the algorithm on training data to obtain proper delays τ for the synergies, and then cross-validate by running the algorithm with the same fixed delay parameters, τ, on test data. Then we can directly compare the rShiftNMF fit results with NMF, since they utilize the same free parameters (after fixing τ).

To avoid overfitting, we also do four-fold validation of the muscle synergies. We run the rShiftNMF algorithm on training data, then fix *both* the activation pattern W and delays τ, and run the same algorithm on four sets of test data. We do the same for the NMF algorithm, fixing just the activation pattern W. This discourages overfitting to the data.

C. Estimating the Number of Muscle Synergies

Note that in the muscle synergy extraction formulation (Equation 3), the number of muscle synergies D must be predefined. Most work on muscle synergies utilize the *variance accounted for* (VAF) metric defined below to estimate the proper number of muscle synergies [15]–[19]:

$$VAF = 1 - \frac{1}{N} \sum_{n=1}^{N} \left(\frac{\|EMG^{(n)} - \sum_{d=1}^{D} W_{n,d} H_{d,t-\tau_{n,d}}\|^2}{\|EMG^{(n)}\|^2} \right),$$

where n indexes each muscle. This is a measure of how well the muscle synergies reconstruct the underlying EMG activity. In the NMF formulation, we have $\tau = 0$ (no delays).

Typically the number of synergies is defined as the minimum D such that the VAF passes some threshold. However, the number of synergies will depend on many factors like the threshold used or the pre-process filtering of the EMG [36], [37]. Other work has attempted to improve on these methods by cross-validating over several trials [38], or utilizing different likelihood measures and information criteria [22].

In this work, we utilize the following 2-step method to determine the number of muscles synergies, similar to the procedure in [38]:

- Determine the number of synergies by thresholding the slope of the VAF curve. For the threshold, we preliminarily set the number of synergies once the VAF increases by less than 0.15. This cutoff was chosen by visual inspection of the trends in the VAF curve.
- Validate the result by looking at the muscle activation patterns, W, of the synergies across different intervals of the patient's EMG, and see if they are consistent (i.e. the dot product between them is greater than 0.9). If they are consistent, we accept the number of muscle synergies to be correct. Otherwise, we lower the synergy number.

This procedure robustly identifies the number of synergies present by using both thresholding and cross-validation.

III. Results

A. Analysis of SCI Patient EMG Activity

1) Improvement in Synergy Extraction With rShiftNMF: We extracted muscle synergies from the EMG activity of the SCI patients using rShiftNMF (to obtain CDSS) as well as NMF (to obtain SS). As discussed in Section II-B, delays in muscle activation between muscle groups are prominent in paraplegics undergoing SCS-induced standing (illustrated in Fig. 3a).

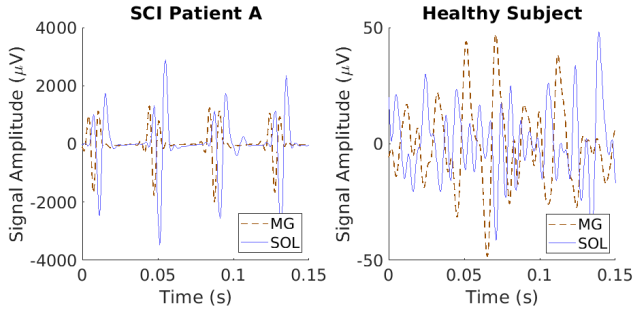

Fig. 3. (Left) Exemplary EMG traces for MG and SOL muscles for SCI patient under spinal stimulation. Note that EMG activity is highly structured and periodic. Furthermore, MG and SOL have similar waveforms, with SOL activated slightly after MG. (Right) Exemplary EMG traces for MG and SOL muscles measured from a healthy subject. EMG activity is more variable without structured delays.

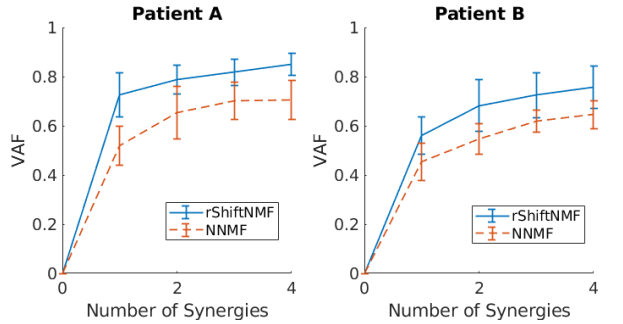

Fig. 4. The variance accounted for (VAF) plotted against the number of synergies extracted. In all cases, VAF was computed using 4-fold validation (i.e., tested on 4 different test sections of the EMG) with fixed delay, τ, and activation pattern, W. For each plot, the VAF with the rShiftNMF algorithm was compared to the VAF with the NMF algorithm. (Left) Results for patient A; (Right) Results for patient B.

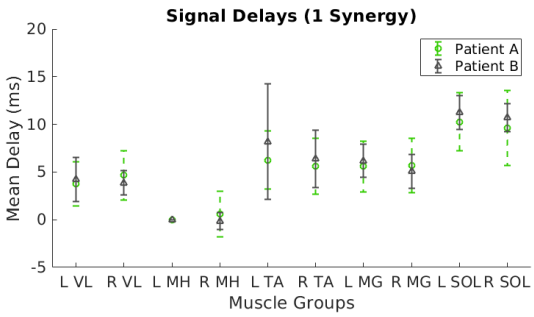

(a)

1 Synergy

	Synergy 1 (All)	Synergy 1 (SSCA)
L VL	4 ± 2	-4 ± 6
R VL	4 ± 3	-2 ± 8
L MH	0 ± 0	0 ± 0
R MH	1 ± 2	7 ± 12
L TA	6 ± 3	-4 ± 8
R TA	6 ± 3	-4 ± 9
L MG	6 ± 3	-5 ± 9
R MG	6 ± 3	-4 ± 8
L SOL	10 ± 3	0 ± 9
R SOL	10 ± 4	0 ± 9

2 Synergies

	Synergy 1 (All)	Synergy 2 (All)	Synergy 1 (SSCA)	Synergy 2 (SSCA)
L VL	11 ± 56	1 ± 115	10 ± 20	0 ± 17.8
R VL	2 ± 77	19 ± 119	34 ± 32	25 ± 40.0
L MH	0 ± 0	0 ± 0	0 ± 0	0 ± 0.0
R MH	3 ± 12	9 ± 68	38 ± 42	31 ± 52.8
L TA	0 ± 84	12 ± 63	5 ± 19	–
R TA	8 ± 8	11 ± 65	2 ± 23	–
L MG	5 ± 65	-29 ± 225	6 ± 20	–
R MG	7 ± 7	28 ± 108	6 ± 20	–
L SOL	11 ± 8	23 ± 116	11 ± 20	–
R SOL	6 ± 50	3 ± 122	10 ± 20	–

3 Synergies

	Synergy 1 (All)	Synergy 2 (All)	Synergy 3 (All)	Synergy 1 (SSCA)	Synergy 2 (SSCA)	Synergy 3 (SSCA)
L VL	4 ± 159	25 ± 169	7 ± 168	-1 ± 7	-2 ± 9	65 ± 130
R VL	11 ± 192	23 ± 224	3 ± 173	206 ± 730	-345 ± 343	59 ± 201
L MH	0 ± 0	0 ± 0	0 ± 0	0 ± 0	0 ± 0	0 ± 0
R MH	1 ± 135	15 ± 167	8 ± 174	-54 ± 647	4 ± 8	4 ± 6
L TA	15 ± 117	31 ± 159	20 ± 94	3 ± 3	0 ± 1	1 ± 1
R TA	9 ± 92	23 ± 124	0 ± 49	3 ± 3	2 ± 1	2 ± 2
L MG	-15 ± 169	27 ± 144	2 ± 36	3 ± 2	183 ± 362	3 ± 2
R MG	9 ± 89	35 ± 142	11 ± 67	2 ± 4	125 ± 245	4 ± 3
L SOL	4 ± 175	22 ± 144	-2 ± 118	9 ± 5	5 ± 3	-237 ± 493
R SOL	11 ± 87	27 ± 123	0 ± 75	6 ± 3	5 ± 3	6 ± 2

(b)

Fig. 5. (a) Muscle activation delay for each muscle in the case of 1 muscle synergy (normalized to the left MH). (b) Table of muscle activation delay for different number of synergies. SSCA denote trials in which 2 muscle synergies are active (see Section III-B). In SSCA trials, delays are more in line with expectations in the 2 synergy case. In all other trials, delays better match expectations in the 1 synergy case. Omitted delays indicate that the synergy did not involve those muscles.

Fig. 3b provides a comparison with a healthy subject's EMG, where we notice the absence of well-defined delays.

Muscle activation delays are only accounted for in the rShiftNMF algorithm, so we expect it to better capture low-dimensional muscle synergy structure in the EMG activity. We confirm this by examining the VAF of the EMG using synergies extracted by each algorithm. This is shown in Fig. 4, and we see that rShiftNMF is effective at capturing the EMG activity with few muscle synergies. With cross-validation, a single synergy extracted by rShiftNMF is able to account for $\approx 60\%$ of the variance in the EMG signals, whereas NMF achieves that reconstruction accuracy only with 3-4 synergies. The fact that the performance of rShiftNMF remains high (and significantly better than NMF) with cross-validation suggests that we are able to capture meaningful structure in the EMG activity with few muscle synergies.

One may note that the VAF observed in Fig. 4 is lower than values typically recorded in the literature, which is due to the fact that (1) we retain a much larger frequency spectrum of the EMG signals in pre-processing, and (2) we validate the results across four different EMG intervals. The important features to note are improved performance compared to NMF, and consistency of VAF after cross-validation.

To validate the results of the rShiftNMF algorithm, we check that the algorithm's calculated delays, τ, are consistent with expected conduction delays, as discussed in section II-B. If the delays, τ, were inconsistent with neurophysiology, this would be an indicator that the rShiftNMF algorithm might be fitting to noise in the EMG activity rather than meaningful structure in the CNS. The delays when considering one synergy are shown in Fig. 5a. This is the most relevant case since only one synergy is activated in the vast majority of trials, as will be discussed in Section III-A2. A table showing the delays (and their variation) across all trials when considering different number of synergies is shown in Fig. 5b. The SSCA cases will be discussed in Section III-B, but currently serve to show that in almost all (non-SSCA) cases, computed delays are non-physiological when considering more than one synergy.

Note that left/right muscles within each muscle group have similar delays, and that delays increase as we go from MH to VL to TA/MG to SOL muscles, which reflects an ordering based on distance from the spinal cord. We also note that the observed delays are in line with the order of magnitude delay expected ($\approx$10 ms) as discussed in Section II-B. The consistency of the delays with physiological models is

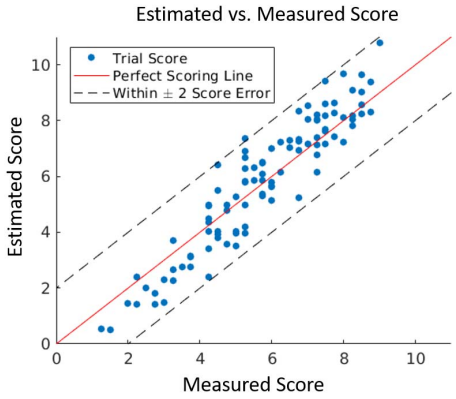

(a)

	Error using All Synergy Features	Error using VAF	Linear Regression with VAF (% trials predicted within ±2)
NNMF	1.21	1.49	69.20%
rShiftNMF	1.12	1.26	76.90%
Prediction Method	Random Forest	Linear Regression	Linear Regression

(b)

Fig. 6. (a) Accuracy in standing score prediction using linear regression with rShiftNMF muscle synergy features and raw EMG power. Measured score is the therapist-graded standing score, and the estimated score is computed by our regression method. (b) Standing score prediction performance based on muscle synergy features only, using scoring scale between 1-10. First and second columns show mean absolute error in score prediction, whereas the third column shows percentage of trials correctly predicted within ±2 of true score.

further evidence that rShiftNMF muscle synergies are capturing physiological phenomena for the SCI patients under SCS that would be missed with muscle synergies extracted by NMF.

For further validation, we looked for correlations between the patient's standing ability and muscle synergy features extracted by rShiftNMF vs. NMF. Recall that therapists provided a score of standing ability, on a scale from 1-10, for each trial (i.e. the measured score). We trained different regression functions (i.e. Random Forest, SVM, linear functional) to see if we could predict the resulting standing score based on muscle synergy features. We found that for patient A, muscle synergy features extracted by rShiftNMF were more strongly correlated with functional performance than synergy features extracted by NMF. We did not repeat the analysis with patient B due to the small number of trials (15) and lower variance in standing scores (e.g. smaller score range from 3-8).

Fig. 6a shows prediction accuracy based on linear regression with EMG power and rShiftNMF muscle synergy features. Using these features to estimate patient standing scores, we found that 97% were within ±2 of the therapist-measured score. In comparison, if we did not include the muscle synergy features, only 91% were within ±2 of the measured score. Fig. 6b compares score classification accuracy – ability to distinguish independent standing (score ≥ 6) from non-independent standing – using synergy features from either NMF or rShiftNMF and 3-fold cross-validation. The results indicate stronger correlation with rShiftNMF muscle synergy features compared to NMF synergy features. Thus adding rShiftNMF synergy features leads to significant improvements in prediction accuracy.

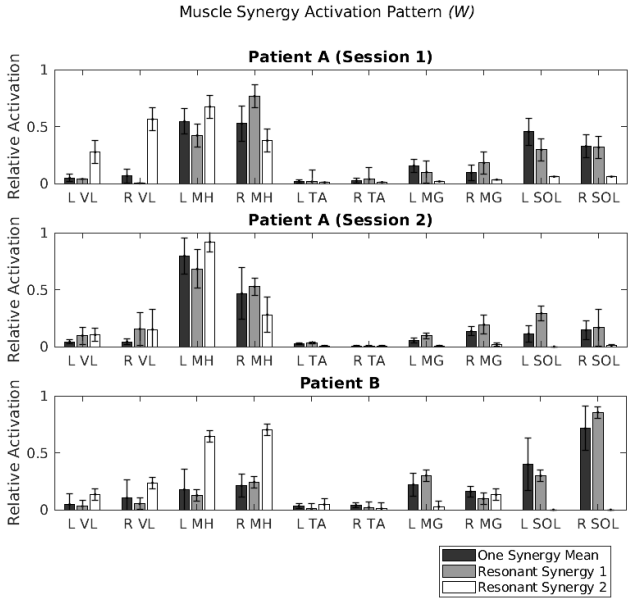

Fig. 7. Comparison of mean activation pattern for non-SSCA trials (single synergy - black bar) with activation patterns for synergy 1 (grey bar) and synergy 2 (white bar) of SSCA trials. Note that the confidence intervals for the synergy 1 activation pattern in the SSCA trials overlaps with the activation pattern of the non-SSCA trials. *(Top)* Patient A (Session 1); *(Middle)* Patient A (Session 2); *(Bottom)* Patient B.

These prediction results, combined with the accurate modeling of physiological delays and significantly improved EMG reconstruction, suggest that rShiftNMF (i.e. CDSS) provides a more useful and physiological description of muscle synergies for SCI patients under SCS. Therefore, for the rest of this section, we use muscle synergies to refer to CDSS.

2) Motor Activity Through Single Synergy Activation: Utilizing the methodology described in Section II-C, we calculated that for 96% of trials (all trials using fixed stimulation pattern), only one muscle synergy was activated during patient standing under SCS. The muscle activation pattern, W, for this synergy was relatively stable (see black bars in Fig. 7). Our results suggest that SCS influences standing ability (i.e. muscle activity) by activating/manipulating this muscle synergy.

Based on these results, one might argue that the activated muscle synergy arises simply due to direct stimulation of dorsal roots with conduction delays to the muscles. However, by looking at cases where a second muscle synergy is activated, the following section provides support that SCS can activate neural circuits beyond the dorsal roots.

B. Activation of Additional Synergy With SCS

For 4 of the 109 trials for patient A and 1 of the 15 trials for patient B, we found two distinct and consistent muscle synergies were active during patient standing under SCS (using same methodology in section II-C). We found that these trials where 2 synergies were active also corresponded to the highest performance trials *and* occurred when, and only when, the patient was stimulated with interleaving stimulation patterns (as described in section II-A.1) rather than a single fixed stimulation pattern. In this section, we argue that the interleaving stimulation achieves *selective spinal circuit activation* (SSCA) of a second spinal circuit (i.e. muscle synergy).

We will refer to the trials with 2 synergies activated as SSCA trials.

First, we show that for the SSCA trials, the activation pattern, W, is distinct for the two muscle synergies – the first synergy is the same muscle synergy common to all the non-SSCA trials, and the second muscle synergy is distinct from the first. Fig. 7 compares the mean activation pattern for the muscle synergy from non-SSCA trials, to the activation pattern of the two muscle synergies from the SSCA trials. We find that the first muscle synergy from the SSCA trials aligns with the muscle synergy extracted from the non-SSCA trials (with respect to the activation pattern W) – mainly activating the medial hamstring and lower leg muscles (MH, MG and SOL). The second synergy primarily activates the VL/MH muscle groups, showing a distinct pattern from synergy 1.

We tested the statistical significance of this hypothesis using a permutation test based on minimum statistical energy developed in [39]. We calculated the p-value corresponding to the hypothesis that the first synergy activation pattern from the SSCA trials matches the synergy activation pattern from the non-SSCA trials, and found that $p = 0.23$ for patient A session 1, $p = 0.11$ for patient A session 2, and $p = 0.64$ for patient B. We *cannot* reject the hypothesis that the activation patterns come from the same distribution at the 10% confidence level. However, if we consider the second muscle synergy from the SSCA trials, we *can* reject the hypothesis that it comes from the same distribution as the muscle synergy of the non-SSCA trials; we compute p-values of $p = 0.01$ for patient A session 1, $p = 0.02$ for patient A session 2, and $p = 0.06$ for patient B. These results suggest that the interleaving stimulation introduces a distinct second muscle synergy (responsible for a complementary set of muscles) during patient standing, while also activating the original muscle synergy.

We must note that since MH is activated significantly by both synergies 1 and 2, its activation level within each synergy may change across runs of the rShiftNMF algorithm. This is because there are different ways to equivalently split the MH activity between synergies 1 and 2. The relative activation of the other muscles is stable across runs.

The introduction of the second muscle synergy (activating the VL/MH muscles) increases the complexity of the muscle activity, requiring the composition of 2 neural commands instead of 1. Fig. 8 illustrates this increased complexity through an additional muscle synergy. In the SSCA trials, the 2^{nd} synergy introduces a significant (in amplitude) and different "basis signal", which allows the spinal cord to generate more complex muscle activity. In contrast, for the non-SSCA trials, if we attempt to extract two synergies by the rShiftNMF algorithm, the 2^{nd} synergy barely contributes to the muscle activity and its waveform significantly mirrors the 1^{st} synergy (see Fig. 8), essentially becoming a redundant synergy. This is also reflected by the marginal increase in VAF seen in the non-SSCA trials from adding a second synergy.

It is important to note that the therapist-rated standing scores were highest for the SSCA trials (the score was $\geq$ 8.75 for all SSCA trials). Therefore, activation of the 2^{nd} muscle synergy (corresponding to a separate neural circuit) *is critical to independent standing* in stimulated SCI patients.

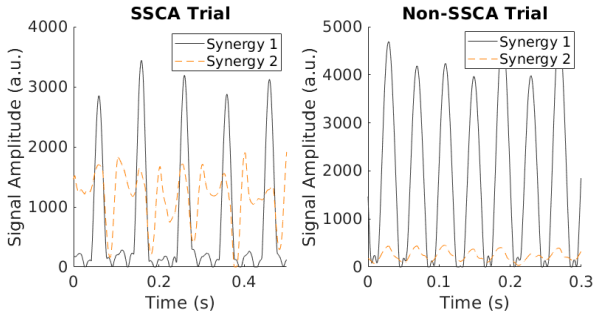

Fig. 8. Representative illustration of synergy activation waveform, H, for SSCA trials vs. non-SSCA trials. Note that in SSCA trials (left plot), the synergy 2 activation waveform plays a significant role in composing EMG activity. In non-SSCA trials (right plot), adding a second synergy results in an activation waveform that is similar to the synergy 1 activation waveform with much smaller amplitude.

1) Controlling for Experimental/Stimulation Differences: Recall that for the SCI experiments, all measurements were taken from the same groups of muscles using the same procedure, with the patients attempting the same biomechanical task (standing). Therefore, we can attribute activation of the additional muscle synergy to the changes in stimulation.

Furthermore, each stimulation pattern within the interleaving stimulation sequences was also tested as a fixed stimulation pattern. However, we never activated the second muscle synergy in the fixed stimulation cases, even using the same stimulation patterns from the interleaving stimulation sequences. Therefore, utilization of the time-varying (interleaving) combination of stimuli dictates activation of the second synergy – not the stimulation pattern of the electrode array. This suggests that SCS is not only stimulating dorsal roots, but also activating neural circuits in the spinal cord. Otherwise we would expect to see the muscle activation pattern, W, depend directly on the stimulation pattern (i.e. stimulation site).

2) Spinal Activation Mapping: Next, we mapped the EMG activity for each muscle synergy to regions of the spinal cord. Based on charts collected in Kandel *et al.* [40], we mapped muscle activity to spinal cord segments and calculated the resulting activation of each spinal segment from each muscle synergy. Fig. 9(a) shows the approximate mapping of the muscle synergies to the spinal cord for the non-SSCA trials and SSCA trials for both patients. For the visualization, we have excluded the MH muscle group since it is activated significantly by both muscle synergies. We see that the first synergy for the SSCA trials and only synergy for the non-SSCA trials maps to the lower lumbo-sacral spinal cord region (≈L5-S2), whereas the second synergy for the SSCA trials maps to the upper lumbo-sacral spinal cord (≈L2-L4). Thus we can interpret the effect of the interleaving spinal stimulation (for SSCA trials) as activating a separate, previously dormant neural circuit in the spinal cord, which modulates motor pools approximately in the upper lumbo-sacral spinal cord.

The muscle synergies are visualized in Fig. 9(b), where we see the 2^{nd} synergy activates motor pools in a higher region of the spinal cord, which is critical to good, stable standing.

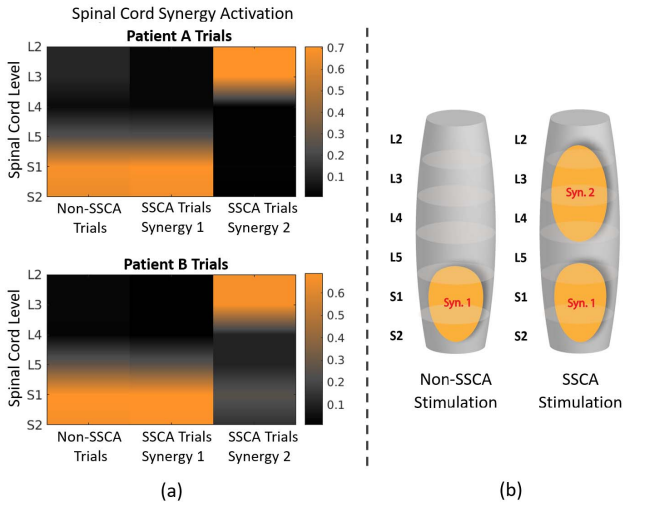

Fig. 9. (a) Visualization of activation of spinal cord regions resulting from each muscle synergy's activation. The left region represents spinal activation of the muscle synergy from non-SSCA trials. The middle region represents spinal activation of the first muscle synergy from the SSCA trials, whereas the right region represents spinal activation of the second muscle synergy from the SSCA trials. (b) Visualization of approximate spinal cord regions activated by each muscle synergy for SSCA trials (on the right) and non-SSCA trials (on the left).

3) Validation With Artificially Imposed Delays: One concern we address here is whether the rShiftNMF algorithm extracts meaningful muscle synergies rather than overfitting to muscle activation delays. In other words, we want to show that the differences between muscle synergies (and the number of muscle synergies) do *not* arise as artifacts of the computed conduction delays, τ, but rather come from the structure in the EMG waveform and muscle activation pattern. To do this, we ran experiments adding artificial delays to different muscles in the data (e.g. swapping the delays between VL and SOL).

In these simulations, the rShiftNMF algorithm successfully captures the modifications in the delays, τ (i.e. the results in Fig. 5 change to account for artificially introduced shifts). We also find that the activation pattern, W, activating signal, H, and computed number of muscle synergies remain very similar (i.e. Figures 7, 8, and 9 remain very similar) after swapping/modifying muscle activation delays, τ. This indicates that extracted muscle synergies arise from meaningful structure in the EMG waveform, and are not artificial artifacts arising from computed conduction delays. As a more concrete example, the VL/MH muscle synergy (i.e. second synergy) is extracted based on the EMG structure, regardless of whether the muscle activations are artificially delayed or shuffled.

4) Biomechanics of SCI Standing Under Stimulation: Note that the muscle synergy activation pattern, W (seen in Fig. 7), is similar for both SCI patients. This inter-patient consistency is in line with previous work showing that muscle synergies are reasonably robust across healthy subjects [41], and suggests that the synergies serve important biomechanical functions.

Interestingly, the muscle synergy activation pattern for the SSCA trials for both patients are not only similar to each other, but consistent with principles for maximally efficient (minimum required torque) stable standing. The authors in [42] found that maximally efficient stable standing should utilize

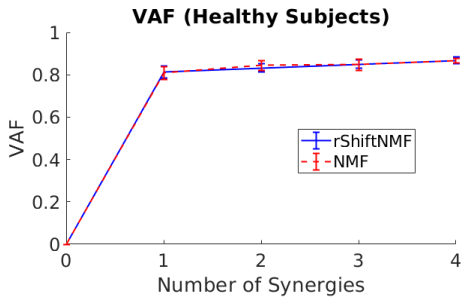

Fig. 10. The VAF plotted against number of synergies extracted for healthy subjects using rShiftNMF vs NMF. The mean VAF across all subjects for a given synergy number was used for each data point. Synergies were cross-validated with fixed delay, τ, and activation pattern, W (or just W for NMF).

2 muscles for knee flexion/extension, 2 muscles for ankle dorsiflexion/plantarflexion, 1 muscle for hip abduction/adduction, and 1 muscle for hip flexion/extension. This is consistent with the SSCA trials, where VL/MH serve as two muscles for knee flexion/extension (and MH can provide hip extension), MG/SOL serve as two muscles for ankle dorsiflexion/plantarflexion, and TA is not active. Synergy 2 likely serves to stiffen the knee joint by proper co-activation of MH and VL. Furthermore, [43] found that TA muscle activity in healthy elderly individuals surprisingly *decreases* postural steadiness in standing, which is consistent with the SCI patients under SCS exhibiting no TA activation.

These results allow us to hypothesize that (after stand training in the clinic) stimulated SCI patients attempt maximally efficient stable standing. In the SSCA trials, SCI standing activates muscle patterns that are maximally efficient for stable standing, and activation of the second muscle synergy is crucial to activate the two necessary muscles for knee flexion/extension. However, in the non-SSCA trials, stable standing is not as well achieved because the absence of the second synergy leads to only one of the two necessary muscles for knee flexion/extension being active.

Due to the limited number of muscles we measured from and limited sample size, we cannot make a strong statement about the biomechanics arising from muscle synergy activation. However, the consistency of our results with prior literature suggests that this hypothesis is worth further exploration.

C. Comparison With Healthy Subject Muscle Synergies

We briefly look at EMG activity from five healthy subjects during quiet standing, and utilize NMF and rShiftNMF to look for muscle synergy structure. From Fig. 10 we see that a single cross-validated muscle synergy reconstructs about 80% of EMG activity, and we compute that a single synergy is activated in each patient using our previous methodology. More importantly, we note that rShiftNMF does *not* perform better than standard NMF under cross-validation. In fact the muscle activation pattern, W, extracted using either method is virtually the same. Therefore, it seems that incorporation of delays, τ, is not necessary nor desirable when extracting muscle synergies from healthy subjects. In other words, healthy subjects utilize synchronous synergies (SS) rather than CDSS.

We also found that the muscle activation pattern, W, for the healthy subjects is significantly different from both SCI patients (for fair comparison, we re-ran analysis for the SCI patient utilizing only the set of 8 muscles common to all patients/subjects). For every patient/subject, the dot product $W_{health} \cdot W_{SCI} < 0.6$ (where $W_{health} \cdot W_{SCI} = 1$ would indicate a perfect match). Thus, the SCI muscle synergies differ substantially from healthy subject synergies not only in synchronization of signal delays, but in the pattern of muscle activation during standing. Therefore, while some form of muscle synergies are present in SCI patients, they are significantly modified (or excited differently) from healthy subject synergies due to spinal injury/stimulation.

IV. Discussion

A. Potential Factors Influencing Muscle Synergy Features

Prior work has shown that the number of extracted muscle synergies can depend on the biomechanical constraints of the task [44], as well as the recorded muscles [37]. We note that during the experiments, all measurements were taken consistently with the same group of muscles, with the patients attempting the same standing task. In this way, while measurement biases and biomechanical constraints may influence the properties of the individual extracted muscle synergies, these factors should not significantly impact the analyses comparing across different trials and patients. In particular, activation of the additional muscle synergy using interleaving stimuli was realized under the *same biomechanical constraints with the same recorded muscles* as all other trials, indicating that spinal stimulation was key in influencing the change in motor activity.

B. Note on Additional Synergy From Interleaving Stimulation

We claim that interleaving spinal stimulation (i.e. time-varying stimuli) during SCI patient standing leads to activation of an additional neural circuit (i.e. a second muscle synergy), which significantly improves patient standing ability. Within our dataset, all cases of interleaving stimulation led to activation of two muscle synergies, whereas all cases of fixed stimulation led to activation of the same single synergy. The results in this study suggest that interleaving stimulation directly leads to activation of important additional muscle synergies. *How* the interleaving stimulation achieves this remains an open question, and learning this mechanism will be important in enabling us to selectively activate other synergies.

Our results are reminiscent of the animal experiments described in Section I, where stimulation at different sites of the animal's spinal cord led to activation of muscle synergies, and co-activation of those sites often led to a linear combination of those muscle synergies. While other studies have relied on post-processing EMG activity to look for muscle synergies in human EMG data, the fact that we are able to mirror the synergy phenomenon in [1], [10]–[12] with humans (activate and combine synergies through spinal stimulation) provides further evidence of the encoding of (potentially modified) muscle synergies in the human spinal cord after SCI.

Furthermore, studies have hypothesized that neurological injury/disease leads to a decrease in the number of muscle synergies activated when composing muscle activity [7], [19], [45], [46]. These prior efforts suggest that synergies may be "merged" after injury. *However*, the fact that proper stimulation activated an additional muscle synergy suggests that muscle synergies are still encoded in the spinal cord after SCI. Hence, we hypothesize that spinal injury impairs the ability of the CNS to activate muscle synergies, even though those neural circuits remain sufficiently intact to be activated by SCS. Recovery of synergy activity after stroke using functional electrical stimulation has been explored [47], though our study looks at re-activating and utilizing existing neural circuitry.

Note that these muscle synergies *may not be* the same synergies present in healthy subjects – they may be pathological, differing from healthy muscle synergies due to the patient's spinal cord injury and intense training in the clinic. However, our results show that some form of muscle synergies are still encoded in the human spinal cord after SCI.

V. Conclusion

This is the first human study analyzing muscle synergies in SCI patients under SCS, and our results shed light on muscle synergies as a key physiological mechanism by which SCS generates motor function. We successfully extracted muscle synergies from SCI patients under spinal cord stimulation using a novel algorithm, and provided evidence that muscle synergies are sufficiently intact (to enable standing abilities) in the human spinal cord after SCI *and* can be selectively activated through proper SCS. Patient motor function is heavily influenced through activation of these muscle synergies, and SCI standing ability can be greatly improved through activation of an additional muscle synergy.

The limited number of SCI patients in this study prevents us from making conclusive statements about muscle synergies across the SCI population. However, we believe the consistency of our results (with prior literature and between our patients) is promising, and that these findings will have significant implications for rehabilitation as we better learn how to activate and train critical muscle synergies through targeted neuromodulation and motor training.

Acknowledgment

The authors thank Enrico Rejc, Claudia Angeli, and Susan Harkema for collecting and sharing the SCI dataset.

References

[1] F. A. Mussa-Ivaldi, S. F. Giszter, and E. Bizzi, "Linear combinations of primitives in vertebrate motor control," *Proc. Nat. Acad. Sci. USA*, vol. 91, no. 16, pp. 7534–7538, 1994.

[2] M. C. Tresch, P. Saltiel, and E. Bizzi, "The construction of movement by the spinal cord," *Nature Neurosci.*, vol. 2, pp. 162–167, Feb. 1999.

[3] E. Bizzi, M. C. Tresch, P. Saltiel, and A. D'Avella, "New perspectives on spinal motor systems," *Nature Rev. Neurosci.*, vol. 1, pp. 101–108, Nov. 2000.

[4] S. F. Giszter, "Motor primitives—New data and future questions," *Current Opinion Neurobiol.*, vol. 33, pp. 156–165, Aug. 2015.

[5] E. Bizzi and V. C. K. Cheung, "The neural origin of muscle synergies," *Frontiers Comput. Neurosci.*, vol. 7, p. 51, Apr. 2013.

[6] W. J. Kargo and S. F. Giszter, "Individual premotor drive pulses, not time-varying synergies, are the units of adjustment for limb trajectories constructed in spinal cord," *J. Neurosci.*, vol. 28, no. 10, pp. 2409–2425, Mar. 2008.

[7] V. C. Cheung *et al.*, "Muscle synergy patterns as physiological markers of motor cortical damage," *Proc. Nat. Acad. Sci. USA*, vol. 109, no. 36, pp. 14652–14656, 2012.

[8] W. J. Kargo and S. F. Giszter, "Rapid correction of aimed movements by summation of force-field primitives," *J. Neurosci.*, vol. 20, no. 1, pp. 409–426, Jan. 2000.

[9] P. Saltiel, K. Wyler-Duda, A. D'Avella, M. C. Tresch, and E. Bizzi, "Muscle synergies encoded within the spinal cord: Evidence from focal intraspinal NMDA iontophoresis in the frog," *J. Neurophys.*, vol. 85, no. 2, pp. 605–619, 2001.

[10] M. C. Tresch, P. Saltiel, A. D'Avella, and E. Bizzi, "Coordination and localization in spinal motor systems," *Brain Res. Rev.*, vol. 40, nos. 1–3, pp. 66–79, Oct. 2002.

[11] E. Bizzi, V. C. Cheung, A. D'Avella, P. Saltiel, and M. Tresch, "Combining modules for movement," *Brain Res. Rev.*, vol. 57, no. 1, pp. 125–133, Jan. 2008.

[12] D. A. McCrea and I. A. Rybak, "Modeling the mammalian locomotor CPG: Insights from mistakes and perturbations," *Prog. Brain Res.*, vol. 165, pp. 235–253, Jan. 2007.

[13] C. B. Hart and S. F. Giszter, "A neural basis for motor primitives in the spinal cord," *J. Neurosci.*, vol. 30, no. 4, pp. 1322–1336, 2010.

[14] T. Takei and K. Seki, "Spinal interneurons facilitate coactivation of hand muscles during a precision grip task in monkeys," *J. Neurosci.*, vol. 30, no. 50, pp. 17041–17050, Dec. 2010.

[15] S. A. Chvatal, G. Torres-Oviedo, S. A. Safavynia, and L. H. Ting, "Common muscle synergies for control of center of mass and force in nonstepping and stepping postural behaviors," *J. Neurophys.*, vol. 106, no. 2, pp. 999–1015, Jun. 2011.

[16] L. H. Ting and J. M. Macpherson, "A limited set of muscle synergies for force control during a postural task," *J. Neurophys.*, vol. 93, no. 1, pp. 609–613, 2005.

[17] J. L. Allen and R. R. Neptune, "Three-dimensional modular control of human walking," *J. Biomech.*, vol. 45, no. 12, pp. 2157–2163, Aug. 2012.

[18] R. L. Routson, S. A. Kautz, and R. R. Neptune, "Modular organization across changing task demands in healthy and poststroke gait," *Physiol. Rep.*, vol. 2, no. 6, 2014, Art. no. e12055.

[19] D. J. Clark, L. H. Ting, F. E. Zajac, R. R. Neptune, and S. A. Kautz, "Merging of healthy motor modules predicts reduced locomotor performance and muscle coordination complexity post-stroke," *J. Neurophys.*, vol. 103, no. 2, pp. 844–857, Dec. 2009.

[20] A. S. Oliveira, L. Gizzi, D. Farina, and U. G. Kersting, "Motor modules of human locomotion: Influence of EMG averaging, concatenation, and number of step cycles," *Frontiers Hum. Neurosci.*, vol. 8, p. 335, May 2014.

[21] D. D. Lee and H. S. Seung, "Algorithms for non-negative matrix factorization," in *Proc. Adv. Neural Inf. Process. Syst.*, Oct. 2001, pp. 556–562.

[22] M. Tresch, V. Cheung, and A. D'Avella, "Matrix factorization algorithms for the identification of muscle synergies: Evaluation on simulated and experimental data sets," *J. Neurophys.*, vol. 95, no. 4, pp. 2199–2212, Apr. 2005.

[23] S. Harkema *et al.*, "Effect of epidural stimulation of the lumbosacral spinal cord on voluntary movement, standing, and assisted stepping after motor complete paraplegia: A case study," *Lancet*, vol. 377, pp. 1938–1947, Jun. 2011.

[24] E. Rejc, C. Angeli, and S. Harkema, "Effects of lumbosacral spinal cord epidural stimulation for standing after chronic complete paralysis in humans," *PLoS ONE*, vol. 10, no. 7, 2015, Art. no. e0133998.

[25] E. Rejc, C. A. Angeli, N. Bryant, and S. J. Harkema, "Effects of stand and step training with epidural stimulation on motor function for standing in chronic complete paraplegics," *J. Neurotrauma*, vol. 34, no. 9, pp. 1787–1802, May 2016.

[26] M. L. Gill *et al.*, "Neuromodulation of lumbosacral spinal networks enables independent stepping after complete paraplegia," *Nature Med.*, vol. 24, no. 11, p. 1677, Nov. 2018.

[27] C. A. Angeli *et al.*, "Recovery of over-ground walking after chronic motor complete spinal cord injury," *New England J. Med.*, vol. 379, no. 13, pp. 1244–1250, Sep. 2018.

[28] N. Wenger *et al.*, "Spatiotemporal neuromodulation therapies engaging muscle synergies improve motor control after spinal cord injury," *Nature Med.*, vol. 22, no. 2, pp. 138–145, 2016.

[29] R. Cheng and J. W. Burdick, "Extraction of muscle synergies in SCI patients," in *Proc. IEEE/EMBC Int. Eng. Med. Biol. Conf.*, Honolulu, HI, USA, Jul. 2018, pp. 17–21.

[30] Y. Sui and J. W. Burdick, "Correlational dueling bandits with application to clinical treatment in large decision spaces," in *Proc. IJCAI Int. Conf. Artif. Intell.*, Aug. 2017, pp. 2793–2799.

[31] Y. Sui, A. Gotovos, J. Burdick, and A. Krause, "Safe exploration for optimization with Gaussian processes," in *Proc. Int. Conf. Mach. Learn.*, vol. 37, Jun. 2015, pp. 997–1005.

[32] S. Muceli, N. Jiang, and D. Farina, "Extracting signals robust to electrode number and shift for online simultaneous and proportional myoelectric control by factorization algorithms," in *Proc. IEEE Trans. Neural Syst. Rehabil. Eng.*, May 2014, pp. 623–633.

[33] A. D'Avella, P. Saltiel, and E. Bizzi, "Combinations of muscle synergies in the construction of a natural motor behavior," *Nature Neurosci.*, vol. 6, no. 3, p. 300, Mar. 2003.

[34] A. D'Avella, L. Fernandez, A. Portone, and F. Lacquaniti, "Modulation of phasic and tonic muscle synergies with reaching direction and speed," *J. Neurophys.*, vol. 100, no. 3, pp. 1433–1454, Sep. 2008.

[35] M. Morup, K. H. Madsen, and L. K. Hansen, "Shifted non-negative matrix factorization," in *Proc. IEEE Workshop Mach. Learn. Signal Process.*, Aug. 2007, pp. 139–144.

[36] F. Hug, N. A. Turpin, S. Dorel, and A. Guével, "Smoothing of electromyographic signals can influence the number of extracted muscle synergies," *Clin. Neurophys.*, vol. 123, no. 9, p. 1895, 2012.

[37] K. M. Steele, M. C. Tresch, and E. J. Perreault, "The number and choice of muscles impact the results of muscle synergy analyses," *Frontiers Comput. Neurosci.*, vol. 7, p. 105, Aug. 2013.

[38] Y. Kim, T. C. Bulea, and D. L. Damiano, "Novel methods to enhance precision and reliability in muscle synergy identification during walking," *Frontiers Hum. Neurosci.*, vol. 10, p. 455, Sep. 2016.

[39] G. J. Székely and M. L. Rizzo, "Energy statistics: A class of statistics based on distances," *J. Stat. Planning Inference*, vol. 143, no. 8, pp. 1249–1272, Aug. 2013.

[40] E. R. Kandel, J. H. Schwartz, T. M. Jessell, S. A. Siegelbaum, and A. Hudspeth, *Principles of Neural Science*, vol. 3, 5th ed. New York, NY, USA: McGraw-Hill, 2014.

[41] G. Torres-Oviedo and L. H. Ting, "Muscle synergies characterizing human postural responses," *J. Neurophys.*, vol. 98, no. 4, pp. 2144–2156, Oct. 2007.

[42] J. Y. Kim, J. K. Mills, A. H. Vette, and M. R. Popovic, "Optimal combination of minimum degrees of freedom to be actuated in the lower limbs to facilitate arm-free paraplegic standing," *J. Biomech. Eng.*, vol. 129, no. 6, pp. 838–847, Dec. 2007.

[43] A. H. Vette, D. G. Sayenko, M. Jones, M. O. Abe, K. Nakazawa, and K. Masani, "Ankle muscle co-contractions during quiet standing are associated with decreased postural steadiness in the elderly," *Gait Posture*, vol. 55, pp. 31–36, Jun. 2017.

[44] F. D. Groote, I. Jonkers, and J. Duysens, "Task constraints and minimization of muscle effort result in a small number of muscle synergies during gait," *Frontiers Comput. Neurosci.*, vol. 8, p. 115, Sep. 2014.

[45] J. Roh, W. Z. Rymer, E. J. Perreault, S. B. Yoo, and R. F. Beer, "Alterations in upper limb muscle synergy structure in chronic stroke survivors," *J. Neurophys.*, vol. 109, no. 3, pp. 768–781, 2013.

[46] L. Gizzi, J. F. Nielsen, F. Felici, Y. P. Ivanenko, and D. Farina, "Impulses of activation but not motor modules are preserved in the locomotion of subacute stroke patients," *J. Neurophys.*, vol. 106, no. 1, pp. 202–210, 2011.

[47] S. Ferrante *et al.*, "A personalized multi-channel FES controller based on muscle synergies to support gait rehabilitation after stroke," *Frontiers Neurosci.*, vol. 10, p. 425, Sep. 2016.